

Collapse Dynamics of Single Proteins Extended by Force

Ronen Berkovich,[†] Sergi Garcia-Manyes,[‡] Michael Urbakh,^{†*} Joseph Klafter,^{†*} and Julio M. Fernandez^{†*}

[†]School of Chemistry, Tel Aviv University, Tel Aviv, Israel; and [‡]Department of Biological Sciences, Columbia University, New York, New York

ABSTRACT Single-molecule force spectroscopy has opened up new approaches to the study of protein dynamics. For example, an extended protein folding after an abrupt quench in the pulling force was shown to follow variable collapse trajectories marked by well-defined stages that departed from the expected two-state folding behavior that is commonly observed in bulk. Here, we explain these observations by developing a simple approach that models the free energy of a mechanically extended protein as a combination of an entropic elasticity term and a short-range potential representing enthalpic hydrophobic interactions. The resulting free energy of the molecule shows a force-dependent energy barrier of magnitude, $\Delta E = \varepsilon(F - F_c)^{3/2}$, separating the enthalpic and entropic minima that vanishes at a critical force F_c . By solving the Langevin equation under conditions of a force quench, we generate folding trajectories corresponding to the diffusional collapse of an extended polypeptide. The predicted trajectories reproduce the different stages of collapse, as well as the magnitude and time course of the collapse trajectories observed experimentally in ubiquitin and I27 protein monomers. Our observations validate the force-clamp technique as a powerful approach to determining the free-energy landscape of proteins collapsing and folding from extended states.

INTRODUCTION

Understanding the molecular mechanisms of collapse of a single protein in a free-energy funnel is of great interest in biophysics (1–4). The development of single-molecule techniques now permits a detailed examination of the free-energy surface over which a protein diffuses in response to a perturbation (5–7). By combining protein engineering with instruments capable of applying a calibrated force and measuring length of a single molecule, it became possible to study the folding and unfolding of a wide variety of proteins placed under mechanical stress. A key discovery made using force spectroscopy was that the mechanical unfolding of proteins was fully reversible (8,9). Upon reducing the pulling force, an unfolded protein begins to fold from a highly extended conformation that is rare or nonexistent in solution, even in the presence of denaturants. For example, at a typical force of 110 pN, mechanically unfolded ubiquitin proteins extend by >80% of their contour length (~20 nm) (10). By contrast, ubiquitin proteins unfolded chemically in solution by 6 M guanidinium chloride stay compact, with a radius of gyration of only ~2.6 nm (11,12). Hence, during mechanical folding/unfolding reactions proteins traverse regions of the free-energy landscape that have never been explored in solution studies (13). Not surprisingly, force spectroscopy studies of protein folding uncovered novel behavior that had not been observed in proteins free in solution. Indeed, force spectroscopy of single proteins showed large fluctuations, from molecule to molecule, of parameters such as the persistence length of the unfolded protein or the size of the activation energy barrier to unfolding (13,14).

Other manifestations of this variability were uncovered through the use of the force-quench technique, where after unfolding a protein at a high force, the pulling force is abruptly quenched to a low value and the ensuing collapse trajectory of the protein is followed with nanometer resolution (15). The resulting collapse and folding trajectories of ubiquitin polyproteins were continuous and marked by several distinct stages, including a prominent plateau phase (15–17). Furthermore, responding to identical force-quench protocols, ubiquitin polyproteins were never observed to follow the same collapse trajectory (13). These puzzling observations showed that a protein collapsing after a force quench could not be readily described by traditional models of all-or-none hopping between well-defined thermodynamic states. Instead, statistical physics models of thermally driven diffusion over a free-energy surface are more appropriate (18). These observations were challenged by claims that the use of polyproteins in the force-quench experiments caused entropic masking and aggregation of the collapsing proteins (19–22). However, it soon became clear that similar force-quench trajectories could be observed in protein monomers, putting these considerations to rest (16). Moreover, similar to force-quench experiments on proteins (15), those on RNA hairpins also showed collapse trajectories that featured a prominent plateau phase of variable duration, ending in a final contraction that led to the native folded state (23). Thirumalai and colleagues used model systems to examine the collapse trajectories of RNA molecules and proposed that the plateau phase was a generic feature of any polymer in a poor solvent condition placed under a stretching force, and that this phase was the result of a force-dependent entropic barrier created by pulling the ends of the molecule (24). Such a force-dependent energy barrier results from the superposition of the entropic elasticity of the molecule combined with shorter-range enthalpic

Submitted December 18, 2009, and accepted for publication February 26, 2010.

*Correspondence: urbakh@post.tau.ac.il, klafter@post.tau.ac.il, or fernandez@columbia.edu

Editor: Kathleen B. Hall.

© 2010 by the Biophysical Society
0006-3495/10/06/2692/10 \$2.00

doi: 10.1016/j.bpj.2010.02.053

interactions, both of which have been identified as the principal contributors to the free energy of proteins collapsing under force (13,24,25).

Here, we demonstrate that Langevin dynamics captures the physics of an extended polypeptide as it diffuses over a free-energy surface in response to an abrupt change. Langevin dynamics has been used extensively to study the unbinding and rebinding trajectories of bond rupture under force (26,27). We now apply a similar approach to examine the dynamics of an extended protein subjected to a force quench, thus providing an integrated picture of the collapse process of a protein under force, both from the experimental and theoretical viewpoints. Our observations now fully explain the puzzling behavior of proteins folding under force-quench conditions and validate force-clamp spectroscopy as a powerful approach to probing the free-energy landscape of a single protein, a central problem in biology.

MATERIALS AND METHODS

Protein engineering

Ubiquitin and I27 protein monomers were subcloned using the BamHI, BglII, and KpnI restriction sites and cloned into the pQE80L (Qiagen, Valencia, CA) expression vector. Finally, they were transformed into the BLRDE3 *Escherichia coli* expression strain. Proteins were purified by histidine metal-affinity chromatography with Talon resin (Clontech, Mountain View, CA) and by gel filtration using a Superdex 200 HR column (GE Biosciences, Piscataway, NJ) (16).

Force spectroscopy

Force-clamp atomic force microscopy (AFM) experiments were conducted at room temperature using a homemade setup under force-clamp conditions described elsewhere (10). Single proteins were picked up from the surface by pushing the cantilever onto the surface, exerting a contact force of 500–800 pN to promote the nonspecific adhesion of the proteins on the cantilever surface. The piezoelectric actuator was then retracted to produce a set deflection (force), which was set constant throughout the experiment thanks to an external, active feedback (PID) mechanism while the extension was recorded. The feedback response was limited to ~3–10 ms. Our measurements of protein length have a peak-to-peak resolution of ~0.5 nm. Experiments were carried out in a sodium phosphate buffer solution, specifically, 50 mM sodium phosphate (Na_2HPO_4 and NaH_2PO_4) and 150 mM NaCl, pH 7.2.

RESULTS AND DISCUSSION

The most typical AFM experiment consists of directly attaching a polyprotein, composed of 8 or 12 identical tandem repeats, between the tip of a cantilever and a gold-coated substrate. The use of polyproteins is advantageous, because they provide an unambiguous fingerprint and a high rate of data collection (9). Although far more laborious, it is also possible to conduct these studies using single-protein monomers by extending them with short polypeptides at each end, providing handles for attachment to the AFM tip and the substrate (16). The individual folding trajectories of protein monomers, which reproduce the same folding phases encountered in their polyprotein counterparts, greatly

simplify their interpretation and provide a closer comparison with theoretical simulation studies (28). Fig. 1 shows force-quench experiments on single monomers of the I27 and ubiquitin proteins. In these experiments, the unfolding of a protein can be well separated from the collapse and folding reaction, which can be triggered by quenching the pulling force to a low value. For example, a single I27 protein is first exposed to a high stretching force of 120 pN, which after a short dwell time triggers the unfolding of the protein, marked by a step extension of 24 nm (Fig. 1 A, upper trace, star symbol). Then, at 4 s, the stretching force is quenched down to 20 pN and the protein is observed to collapse in several characteristic stages. From similar recordings of the force being quenched down to 10–20 pN, we observed that the first stage

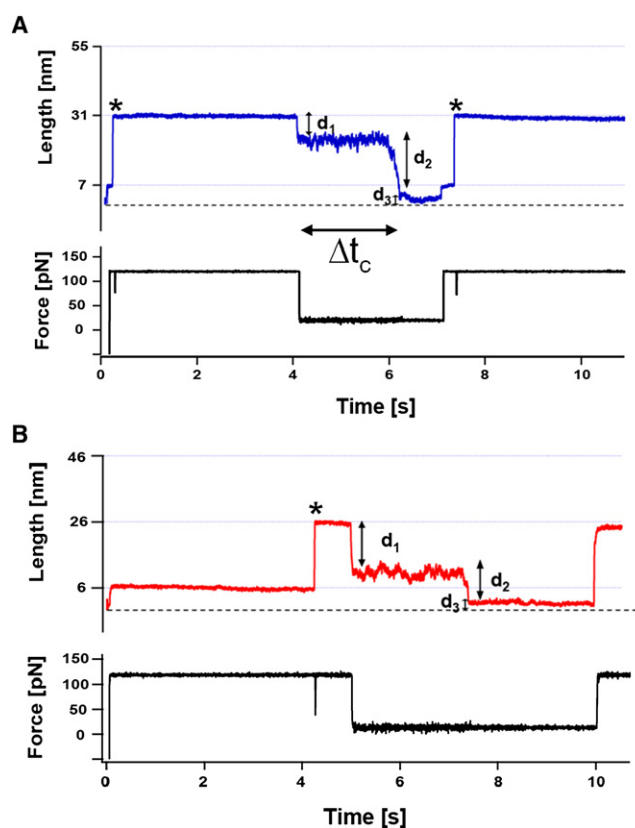


FIGURE 1 Force-clamp experiments on I27 and ubiquitin monomers reveal the time-course evolution of individual collapse trajectories of an extended protein in response to a force quench. (A) An I27 protein monomer unfolds and extends by ~24 nm (upper trace, asterisks) at a high pulling force (lower trace). Upon quenching the force to a low value, F_C , we observed the characteristic collapse behavior that has been observed in both polyproteins and single-protein monomers. The collapse is marked by distinct stages. First, we observe a rapid reduction in length by an amount d_1 , reaching a plateau region of varying duration, Δt_c , which resolves into a final contraction of magnitude d_2 . The fully collapsed state is separated from the surface by a distance d_3 . Another common feature of force-quench recordings is the prominent increase in the magnitude of the end-to-end length fluctuations observed during the plateau stage of the collapse. These fluctuations are smaller in both the extended state and the fully collapsed state. (B) Force-quench experiments on single ubiquitin proteins reveal a very similar collapse dynamics.

corresponds to a recoil of magnitude $d_1 = 11.0 \pm 4.7$ nm ($n = 43$) that occurs concomitantly with the quench, followed by a plateau stage of duration Δt_c , which ends with a collapse of magnitude $d_2 = 17.0 \pm 4.2$ nm ($n = 11$), reaching a final length of $d_3 = 3.3 \pm 2.2$ nm ($n = 40$) for the fully collapsed protein (Fig. 1 A). A similar set of experiments completed with ubiquitin monomers (Fig. 1 B) measured values of $d_1 = 9.2 \pm 4.1$ nm ($n = 31$), $d_2 = 11.8 \pm 3.6$ nm ($n = 11$), and $d_3 = 2.4 \pm 1.7$ nm ($n = 22$). The set of values obtained for ubiquitin are smaller than those measured for the I27 protein, reflecting the smaller size of ubiquitin (76 amino acids versus 89 for I27). After a protein collapsed, a second force pulse back up to 120 pN triggered a second unfolding event, which verified that the protein had effectively refolded. However, sometimes the protein fully collapsed but did not recover its mechanically stable state during the time of the quench (Fig. 1 B). Another characteristic feature of these recordings is the large increase in the size of the end-to-end fluctuations of the protein, apparent during the plateau stage, which rapidly vanish as the protein reaches the fully collapsed stage (Fig. 1, A and B). In all recordings, the value of Δt_c is highly variable and has been shown before to be force-dependent for polyproteins, as well as their monomers, of both I27 and ubiquitin (15,16).

To explain the experimental collapse behavior of an extended protein after a force quench (Fig. 1), we first examine the components of the free energy of the protein. The free energy of an extending protein can be qualitatively rationalized as the combination of at least two distinct components, an entropic term that accounts for chain elasticity and an enthalpic component that includes the short-range interactions arising between the neighboring amino acids as the protein contracts (13). Extending proteins are reasonably well described by the phenomenological wormlike chain (WLC) model of entropic elasticity (29). The WLC model has two independent variables; the contour length of the protein, L_c , and the persistence length, P . The WLC model provides us with the first component of the free energy of an extended protein:

$$U_{WLC} = \frac{k_B T}{P} \left\{ \frac{L_c}{4} \left[\left(1 - \frac{x}{L_c} \right)^{-1} - 1 \right] - \frac{x}{4} + \frac{x^2}{2L_c} \right\}, \quad (1)$$

where k_B is Boltzmann's constant, T is the absolute temperature, and x is the protein length. The use of the WLC model for a description of a nonequilibrium phenomenon like the relaxation dynamics of a semiflexible polymer is an approximation that is justified when the characteristic relaxation time for the polymer dynamics is much shorter than the time for collapse. For the values of the parameters used in our work, the relaxation time estimated using the Rouse time is $\tau_R \sim 0.02$ s, which is at least an order of magnitude smaller than a typical collapse time, $\tau_c \sim 200$ ms. Over the same end-to-end coordinate, x , an applied pulling force, F , changes the free energy of the molecule by an amount

$$U_P = -F \times x. \quad (2)$$

As shown in Fig. 2 A (a), the sum of these two components, $U = U_{WLC} + U_P$, shows a force-dependent minimum, which marks the most probable length of the molecule at a given pulling force. In Fig. 2 A, we calculate that for typical values of $L_c = 30$ nm, $P = 0.4$ nm, and a pulling force of 10 pN, the free energy has a minimum at 13 nm. This minimum solely marks the elastic behavior of the extended polypeptide, and we therefore call it the entropic minimum. We must consider also that as a protein contracts and reduces its end-to-end length, more and more stabilizing interactions among the amino acids in the chain are involved, and the free energy of the polymer is expected to decrease rapidly, creating an enthalpic minimum. A simple educated guess satisfying this condition can be described by the Morse potential:

$$U_M = U_0 \left\{ \left[1 - e^{-\frac{2b}{Rc}(x-Rc)} \right]^2 - 1 \right\}, \quad (3)$$

where U_0 , Rc , and b are Morse parameters that define the depth, position, and spread of the potential well, respectively. Notably, the Morse potential exhibits a well defined minimum larger than zero, which corresponds to the folded length of the protein monomer (Fig. 1, d_3). Fig. 2 A (b) plots a Morse potential evaluated for $U_0 = 100$ pN nm (~ 24 kT), $b = 2$, and $Rc = 4$ nm. The enthalpic minimum at 4 nm described by the Morse potential reflects a molecule that cannot collapse further than its approximate folded length. From these simple considerations, the total free energy of an extended protein is then given by

$$U = U_{WLC} + U_P + U_M. \quad (4)$$

A plot of the total free energy as a function of the end-to-end extension, x , at a pulling force of 10 pN, is shown in Fig. 2 A (c). In a straightforward manner, the total free energy shows two minima, the first at ~ 4 nm and the second at 13 nm. Less obvious is the fact that separating these two minima is a barrier of magnitude $\Delta E = 10.7$ pN nm, which is sufficiently large to trap for some time a collapsing polypeptide before it reaches the deepest minima at 4 nm.

In Fig. 2 B, we examine the changes in free energy triggered by a force quench from 100 pN down to 10 pN. The total free energy at 100 pN shows a pronounced minimum at 25 nm, which is dominant and serves as the starting point of the quench (Fig. 2 B, 1). After the quench, the protein instantaneously switches to the free energy calculated at 10 pN (as in Fig. 2 A), without changing length (Fig. 2 B, 2). The protein then diffuses downhill until it reaches the minimum at 13 nm (Fig. 2 B, 3). Overcoming the activation energy that separates this minimum from the fully collapsed length at 4 nm takes time and many thermal trials. The protein eventually reaches its fully collapsed length at 4 nm, completing the trajectory of the quench (Fig. 2 B, 4). This simple description of the dynamics of a protein undergoing a force quench can be formalized with the overdamped Langevin equation:

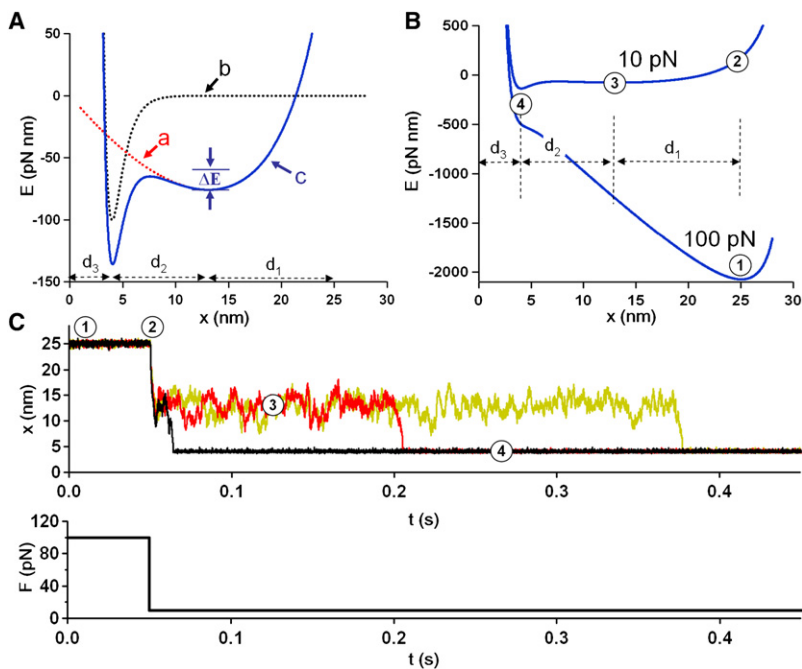


FIGURE 2 Free energy and Langevin dynamics of an extended polypeptide in response to a force quench. (A) Components of the free energy, $E(F, x)$, for a 30-nm-long polypeptide placed under a constant stretching force of 10 pN. The elastic contribution at 10 pN is calculated from the WLC model (a), using a persistence length of $P = 0.4$ nm. The short-range attractive energy is calculated from a simple Morse potential (b) centered at a folded length of 4 nm. The total free energy of the polypeptide at 10 pN is the sum of these two components (c). A distinct energy barrier, ΔE_c , separates the minima of the elastic contribution from the fully collapsed state at 4 nm. (B) Representation of a force quench in the free energy of the extended polypeptide. At 100 pN, $E(x)$ shows a pronounced minimum at ~ 25 nm (1), marking the initial length of the stretched polypeptide. Instantaneously upon quenching the force down to 10 pN, the extension of the polypeptide does not change (1 and 2), but the free energy of the molecule changes abruptly (see also upper trace in A). Then, the molecule rapidly diffuses downhill toward the new minima located at 13 nm (3; see also A). d_1 represents the magnitude of this drop. The molecule now dwells at the 13-nm minimum until, driven by thermal fluctuations, it overcomes the energy barrier seen in A, dropping into the minimum of the Morse potential (4) located at 4 nm. The magnitude of this drop is measured by d_2 . The parameter d_3 measures the fully collapsed length of the polypeptide. (C) Collapse trajectories calculated by solving the Langevin equation for a force quench from 100 pN down to 10 pN using the free energy, $E(x)$, constructed in A and B.

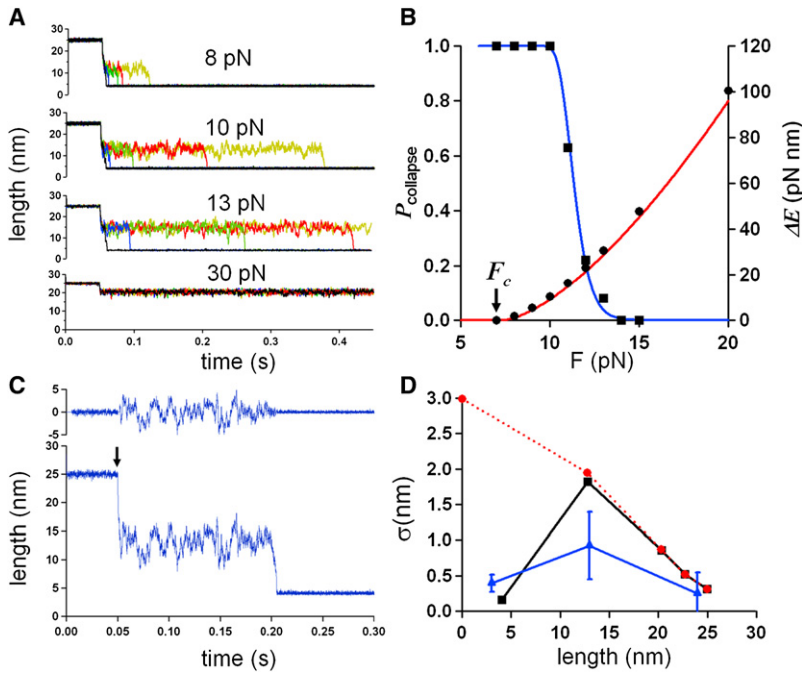
$$\eta \frac{dx}{dt} = \left(\Gamma(t) - \frac{\partial U}{\partial x} \right), \quad (5)$$

where $\Gamma(t)$ is a random force representing the thermal fluctuation, U is the free energy of the protein given by Eq. 4, and η is the friction coefficient, which is related to the diffusion coefficient, D , for protein internal dynamics by $\eta = k_B T / D$. The random force is characterized by a Gaussian distribution with $\langle \Gamma(t) \rangle = 0$ and satisfies the fluctuation-dissipation relation $\langle \Gamma(t) \Gamma(t') \rangle = 2\eta k_B T \delta(t - t')$, in which the angled brackets denote a statistical average over an ensemble of trajectories, and $\delta(t)$ is the Dirac δ function. The random force causes the solutions of this differential equation to be stochastic.

We solved Eq. 5 numerically for a force-quench protocol where the force was abruptly reduced from 100 pN down to 10 pN (Fig. 2 C, lower trace). The solutions to Eq. 5 had the form of trajectories of $x(t)$, three of which are shown in Fig. 2 C. The simulated collapse trajectories accurately capture the principal features of those observed experimentally; a rapid initial collapse followed by a plateau phase, which after a highly variable time ends in a final abrupt contraction. Given that the free energy utilized in the simulation is shown in Fig. 2, A and B, we know precisely what the various stages of collapse correspond to. These stages are labeled 1–4 in Fig. 2 C, and match the corresponding labels in Fig. 2 B. The amplitude of the initial contraction, denoted as d_1 , corresponds to the difference between

the positions of the entropic minima at 100 pN and 10 pN; $d_1 = 12$ nm. After a variable waiting time, the protein then collapses further into the enthalpic minimum at $d_3 = 4$ nm. The lengthscale of this collapse is equal to the difference between the positions of the two minima observed at 10 pN: $d_2 = 9$ nm.

One important observation from the experimental collapse trajectories was that the average duration of the plateau phase (Δt_C in Fig. 1 A) was very steeply dependent on the magnitude of the quenched force (15,16). This is easily reproduced by Langevin dynamics, as shown in Fig. 3 A, where we present several trajectories obtained from force-quench simulations, as described above. In these simulations, the 100-pN initial force was quenched to different values each time. The simulations show that a force quench down to 8 pN triggers a rapid collapse of the protein. At higher quench forces, the duration of the collapse plateau is rapidly increased. Finally, a force quench down to 30 pN elicits only the initial contraction but invariably fails to collapse. The force dependency of the duration of the collapse trajectories results from the force dependency of the energy barrier separating the entropic minima (~ 13 nm at 10 pN) from the enthalpic minima at 4 nm (Fig. 2 A). Fig. 3 B (circles) shows the height of this barrier for different quenching forces. After a critical force, F_c , below which it disappears, the barrier increases rapidly, reaching $\Delta E \sim 24$ kT at 20 pN. This means that at $F > 20$ pN, the energy barrier separating the two minima becomes too high for the thermal environment of the protein to overcome and the



and then drop to a small value reflecting the collapse into the sharp minima of the Morse potential (Fig. 2 A). This behavior is very similar to that observed experimentally for I27 protein monomers (triangles) and contrasts the monotonic increase in the value of σ expected from a free-energy term that lacks the Morse potential (circles).

protein cannot fully collapse. These observations result from a simple inspection of how the free energy changes as a function of the quench force. However, it is desirable to obtain an analytical form for the force dependency of this barrier. Toward this aim, we approximate the potential profile in the vicinity of the barrier by a cubic potential (26,30), obtaining the relation:

$$\Delta E(F) = \varepsilon(F - F_c)^{3/2}, \quad (6)$$

where F_c is the critical force under which the barrier between the entropic and enthalpic minima vanishes and ε is a constant. Both F_c and ε can be expressed analytically in terms of the parameters of the WLC and Morse potentials (see Appendix). For the values of the parameters chosen here, we calculate $F_c = 7.37$ pN and $\varepsilon = 2.14 \sqrt{\text{nm}^2/\text{pN}}$.

A fit of Eq. 6 to the data of Fig. 3 B (solid line) gave values of $F_c \sim 7.05$ pN and $\varepsilon = 2.125 \sqrt{\text{nm}^2/\text{pN}}$, which are quite close to those calculated from the analytical forms. The goodness of the fit demonstrates the validity of the cubic potential approximation and of Eq. 6 at low forces. For large forces, the approximation becomes less accurate (not shown). However, in the system under consideration, the collapse occurs mainly at forces < 20 pN, and for this region, the model describes the force dependency of the barrier rather well (Fig. 3 B).

The mean time to collapse (Figs. 1 and 2 C, Δt_c) is determined by the dwell time in the entropic minimum, set by the

FIGURE 3 Langevin dynamics of a collapsing polypeptide is force-dependent. (A) Sample of collapse trajectories obtained by solving the Langevin equation for quenches down to 8 pN, 10 pN, 13 pN, and 30 pN. The simulations show that the probability of collapse is strongly dependent on the quenched force. (B) The magnitude of the energy barrier to collapse, ΔE (see Fig. 2 A), is force-dependent, as determined directly from the free energy (solid circles). The size of the barrier is well described by $\Delta E = \varepsilon(F_c - F)^{3/2}$ (solid line), with $F_c \sim 7.05$ pN and $\varepsilon = 2.125 \sqrt{\text{nm}^2/\text{pN}}$. Below the critical force, the barrier disappears. As a consequence of the properties of ΔE , the probability of collapse is strongly dependent on the quenched force. $P_{collapse}$ over a quench of $\Delta t_c = 4$ s as a function of the quench force (solid squares) is well

described by $P_{col} = 1 - e^{-(k_0 e^{-\frac{\Delta E(F)}{k_B T}})^{\Delta t}}$, using the same values of F_c and ε . (C) Force-dependent end-to-end fluctuations during a quench. Collapse trajectory calculated using Langevin dynamics for a force quench from 100 pN down to 10 pN (arrow). The amplitude of the fluctuations at each stage was obtained by measuring the deviations from the mean (upper trace). The amplitude of the fluctuations measures the curvature around the energy minima of the free energy, at each force. (D) Standard deviation, σ , of the length fluctuations as a function of the mean extension measured from Langevin dynamics at constant force (squares). The fluctuations reach a maximum at 13 nm

magnitude of ΔE . Thus, the mean time to collapse can be described by the equation

$$\langle \Delta t_c \rangle = \frac{1}{k_0} e^{\frac{\Delta E(F)}{k_B T}}, \quad (7)$$

where $\Delta E(F)$ is given by Eq. 6 and k_0 is the rate of collapse at $F = F_c$. Here, we define this rate as $k_0 \sim 74 \text{ s}^{-1}$. Equations 6 and 7 show that the mean time to collapse depends exponentially on the quenched force, F , a feature which was observed in previous experimental studies (15,16).

From an ensemble of Langevin trajectories calculated numerically at different forces, we can find the probability of complete collapse over a 4-s time window (Fig. 3 B). The simulations show that at 10 pN, all molecules are observed to collapse fully, whereas at 15 pN none do. This is a very steep force dependency. The corresponding analytical form can be calculated as the probability of leaving the entropic minimum and fully collapsing over a given time period, Δt , for a quench force F , given by

$$P_{col} = 1 - e^{-(k_0 e^{-\frac{\Delta E(F)}{k_B T}})^{\Delta t}}. \quad (8)$$

A plot of the analytical Eq. 8 is shown in Fig. 3 B, which readily describes the results of the Langevin simulations, providing a further demonstration of the validity of Eq. 6 for describing the force dependency of the energy barrier separating the entropic and enthalpic minima during a force

quench. Our analysis demonstrates that the experimentally observed force-dependent time course of collapse of an extended protein results from the force-dependent height of the energy barrier separating the entropic and enthalpic minima that forms when the force is applied to a protein.

An important characteristic of the experimental measurement, also reproduced by the Langevin simulations, is the amplitude of the length fluctuations in each region of the collapse trajectory. Fig. 3 C shows a Langevin simulation of a collapse and the noise in each region of the trajectory before the quench; after the quench, while the molecule is trapped in the entropic minima; and after a full collapse into the enthalpic minimum. Fig. 3 D presents the changes in the standard deviation, σ , measured from the fluctuations in length of the simulated trajectories, obtained at each minimum over a range of forces. Langevin simulations using only the contributions to the free energy made by the WLC and the pulling force (Fig. 3 D, circles) show that the variance of the fluctuations at the entropic minimum increases with a decrease in the force and is largest at zero pulling force. This is expected, given that the entropic minimum observed under these conditions becomes shallower as the pulling force is decreased. By contrast, if the full free-energy term is used by adding the contribution of the Morse potential (Eq. 4), the variance, σ , of the fluctuations first increases as before but then is greatly reduced as the protein collapses further to the enthalpic minimum (Fig. 3 D, squares). These results match the trend observed in the fluctuations measured experimentally from I27 proteins (15,16) (Fig. 3 D, triangles). However, in these experiments the limited bandwidth (~ 200 Hz) of the force-clamp apparatus reduces the amplitude of the length fluctuations observed experimentally. Analytically, the variance of the protein length at each minimum (Fig. 2, B and C, 1, 3, and 4) can be estimated as $\sigma = \sqrt{k_B T / |U''_{\min}|}$, where $|U''_{\min}| = |\frac{\partial^2 U}{\partial x^2}|_{x_{\min}}$ defines the curvature (stiffness) of the potential at the minimum. Thus, measurements of the

variance of the protein length, σ , may provide important information on the stiffness of the potential at the minima, $K = U''_{\min}$, and the dependence of the stiffness on the applied force. For example, at 10 pN, the position of the entropic minimum is $x_{\min} = 13$ nm (Fig. 2 A) and the variance measured from the simulations is $\sigma = 1.71$ nm (Fig. 4 B). We can also calculate the potential stiffness as $K = \frac{k_B T}{\sigma^2}$ (31), obtaining a value of $K = 1.42$ pN/nm, which compares well with the stiffness directly measured from the potential, $K = 1.27$ pN/nm.

Analysis of the end-to-end fluctuations of the protein also yields additional information on the collapsing proteins. For example, the effective diffusion coefficient, D , for protein collapse can be estimated from the time evolution of the length fluctuations at any of the free-energy minima. Note that D is different from the diffusion coefficient of the protein in its native state dwelling in a solution: here, it is an inner property that characterizes the given system, which is under a force constraint. Using the Orenstein-Uhlenbeck equation (31) for the time evolution of the mean-square displacement of the trajectories at a potential minimum, $\Delta x(t)^2$, we obtain

$$\begin{aligned} \overline{\Delta x(t)^2} &= \left[\frac{1}{N} \sum_{i=1}^N (x_i(t - t_i) - x_0) \right]^2 \\ &= \sigma^2 \left[1 - \exp\left(-\frac{2Dt}{\sigma^2}\right) \right], \end{aligned} \quad (9)$$

where x_0 is the length of the protein at the minimum, t_i is a time at which the i th trajectory approaches the minimum, and σ is the variance of the length. Averaging is done over an ensemble of N trajectories. At long times, $t \gg \sigma^2/D$, the mean-square deviation, $\Delta x(t)^2$, approaches the asymptotic value σ^2 . The use of this approach to measure D from collapse trajectories is straightforward. For example, applying Eq. 9 to the simulated trajectories of Fig. 3 C, we

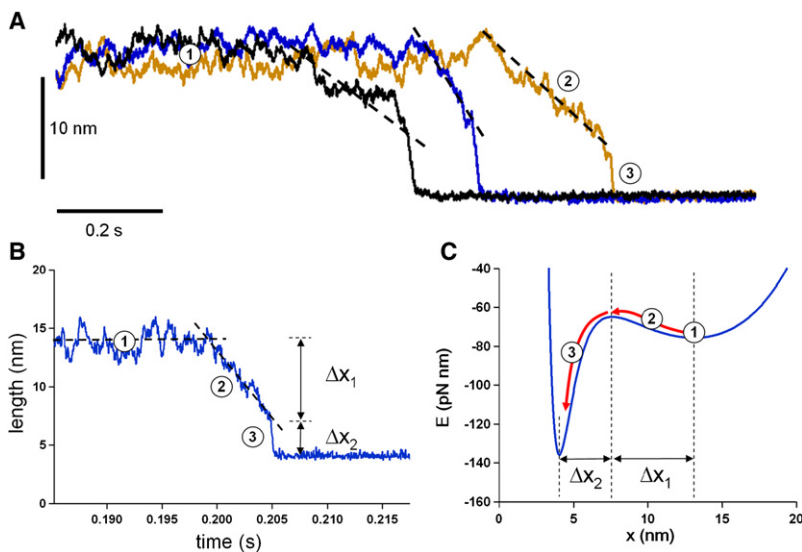


FIGURE 4 Distinct slopes in the final collapse event track the ascending and descending limbs of the energy barrier. (A) One notable feature of the final collapse observed during a force quench is that sometimes, distinct slopes can be distinguished. The figure shows three different experimental traces of single ubiquitin molecules during their final collapse events after a force quench. The traces show that after dwelling for some time at ~ 13 – 16 nm, the collapsing molecules first contracted at a relatively constant rate of 50–100 nm/s, followed by an abrupt increase in the rate of contraction to ~ 500 nm/s. These are common features observed during force quench on ubiquitin polyproteins and monomers. (B) Distinct slopes during the final collapse of a polyprotein are also characteristic of calculated Langevin trajectories. After leaving the free-energy minima located at 13 nm (1), the molecule shortens a distance of $\Delta x_1 = 8.9$ nm by diffusing uphill toward the transition state (2), and then contracts abruptly by a further $\Delta x_2 = 4.5$ nm, completing the collapse of the molecule. (C) Plot of $E(x)$ at 10 pN, identifying the stages of contraction described in B.

measured $D \approx 1500 \pm 220 \text{ nm}^2/\text{s}$, in good agreement with the input value of $D=1500 \text{ nm}^2/\text{s}$. Unfortunately, the reduced bandwidth of our current force-clamp instrumentation ($\sim 200 \text{ Hz}$) prevents us from making use of this approach, which depends on measuring fluctuations at a full bandwidth of at least 5 kHz for comparable values of D . However, our observations certainly invite experimental verification in the near future.

Several additional features of the energy landscape of a collapsing protein can be measured from force-quench trajectories (Fig. 4). For example, a striking feature of the experimentally observed collapse trajectories of polyubiquitin proteins are the abrupt changes in slope observed during the final contraction of the protein after a quench (see Fig. 2 in Fernandez and Li (15)). We now observe similar marked changes in slope during the collapse of single ubiquitin proteins (Fig. 4 A). It is striking that all collapse trajectories obtained using Langevin simulations show the same abrupt changes in the slope during their final contraction (Fig. 4 B), similar in magnitude to those observed experimentally. The origin of these slope changes can be readily identified from the length dependence of the free-energy profile (Fig. 4 C). When the thermally driven final contraction begins, the protein shortens uphill by a distance $\Delta x_1 = 5.5 \text{ nm}$ from the entropic minimum, up to the transition state located at 7.6 nm (Fig. 4 C, 2). This is a diffusion process and the observed slow rate is caused by the uphill shortening, which reduces the driving force for collapse. Therefore, each successful collapse trajectory observed both experimentally and in our simulations is the result of multiple up-and-down dynamics, where the protein attempts to successfully cross the uphill energy barrier. By contrast, after crossing the transition state at 7.6 nm , the protein now shortens downhill under a strong potential bias at a much higher rate and by an amount $\Delta x_2 = 3.6 \text{ nm}$, as it completes the collapse trajectory toward the enthalpic minima located at 4 nm . Thus, the length marking a change in the slope of the final phase of the collapse trajectories defines the position of the barrier's maximum. Due to the stochastic nature of the collapse trajectories, the two distinct slopes that we observe present a degree of variability. This variability notwithstanding, it is remarkable that all experimental and Langevin trajectories that collapse to the enthalpic minimum show the phases illustrated in Fig. 4, A and B. The final rate of collapse over Δx_2 (Fig. 4, B and C) can be used to measure the energy difference between the height of the barrier and the minimum of the enthalpic well:

$$\langle U_{\text{max-min}} \rangle = \frac{k_B T}{D} \frac{1}{N} \sum_i \int_{t_{\text{max}}}^{t_{\text{min}}} \left(\frac{dx}{dt} \right)^2 dt, \quad (10)$$

where the sum is taken over an ensemble of N trajectories and the times t_{max} and t_{min} correspond to the beginning and end of the final collapse slope. All quantities in the right-

hand side of Eq. 10 can be measured experimentally from a small ensemble of collapse trajectories. Applying Eq. 10 to 10 simulated trajectories of force quench between 100 and 10 pN , we obtained an averaged value of $\langle U_{\text{max-min}} \rangle = 75 \text{ pN nm}$, which is in agreement with the input value of 71 pN nm . As before, although it is obvious from the experimental traces (Fig. 4 A), the final collapse stage is rate-limited by the bandwidth of our instrumentation and thus will have to wait for force-quench experiments with a much expanded bandwidth.

Although the resemblance between the collapse trajectories obtained from Langevin simulations and the experimental trajectories is striking, there is still much variation in the experimental data that remains unexplained. For identical force-quench protocols, the amplitudes of the different stages of the collapse vary significantly. In contrast to Langevin simulations, the value of parameters such as d_1 and d_2 , and Δx_1 and Δx_2 , vary noticeably from trace to trace in actual experiments (e.g., Figs. 1 and 4 A). Changes in the value of these parameters are most easily explained by changes in the persistence length of the different collapsing proteins. A puzzling and longstanding observation was that a protein could exhibit very different persistence lengths during extension and collapse. Indeed, the persistence length of the PEVK segment of the giant protein titin was shown to be widely distributed, ranging from 0.25 nm to $>2.5 \text{ nm}$, as revealed by a combined electron microscopy and AFM study (32). In a similar way, ubiquitin polyproteins showed collapse trajectories that were consistent with persistence lengths that varied from molecule to molecule over a similar range (13). An analogous behavior was observed for the case of protein L, which exhibited a distribution of unfolding step sizes when stretched under constant force conditions (33). Thus, persistence length in proteins most likely should be considered to be a parameter that shows static disorder. Consequently, we examined the effect of variations in the persistence length, P , on the free energy of a collapsing protein. Our results are summarized in Table 1. The data show that variations in the persistence length of a collapsing protein affect the free energy in very significant ways. For example, a persistence length of 0.1 nm shifts the value of the critical force up to 23.5 pN . Hence, a force quench down to 10 pN would result in a fast downhill collapse trajectory lacking the plateau phase. In contrast, a persistence length of 2 nm shifts the critical force down to 1.7 pN and increases the collapse barrier ΔE , preventing the full collapse

TABLE 1 Parameters defining the free energy of a protein mechanically stretched at 10 pN of force as a function of the persistence length, P

P (nm)	ΔE (pNnm)	d_1 (nm)	d_2 (nm)	Δx_1 (nm)	Δx_2 (nm)	F_c (pN)
0.1	0	15.4	0	0	0	23.5
0.4	10.4	12	9	5.4	3.6	7
1	57.2	7.5	15.3	12.3	3	3.1
2	95.8	5	18.7	15.8	2.0	1.7

of the protein during a quench to 10 pN. These variations in collapse trajectories are readily observed in force-quench experiments. In a similar way, variations in persistence length readily explain the variations in the values of d_1 , d_2 , Δx_1 , and Δx_2 that are evident in the experimental collapse trajectories.

We have shown here that when we take into account the effect of a pulling force on the free energy over the entire range of extension available to a protein, we can fully account for the different stages of collapse observed during a force-quench experiment. As has been noted already by Thirumalai in his work on RNA hairpins (24), applying force to a molecule causes the appearance of an entropic energy barrier that limits collapse. As demonstrated here using Langevin dynamics, the detailed features of this barrier manifest themselves at each stage of the collapse observed in proteins undergoing a force-quench. Furthermore, as a consequence of the nanometer-long distances to transition state, Δx_1 and Δx_2 , which are a feature of this barrier, the rate of crossing this barrier is steeply force-dependent. This is likely to be the cause of the steep force dependence of collapse that has been observed in AFM experiments for ubiquitin and I27 (13,15,16), as well as in optical tweezers experiments on RNase H (34). The steep force dependence of the refolding kinetics of ubiquitin observed in recent AFM constant-velocity experiments (35) and simulations (36) has also been explained in terms of the entropic elasticity of the unfolded state. Contrary to our observations under force-quench conditions, where we observe a complex, cooperative collapse of the extended protein down to its folded length upon sudden quench of the pulling force (15,16), the experiments under constant-velocity conditions revealed a simple two-state folding transition for each individual ubiquitin domain. As pointed out by Thirumalai (24), these seemingly contradictory conclusions can nevertheless be rationalized in terms of the different experimental conditions applied in the two cases. In constant-velocity experiments, the ubiquitin protein was pulled at a very low speed, thus sampling near-equilibrium conditions at each particular moment of the refolding trajectory. By contrast, in our force-quench scenario, the protein is brought suddenly from an extended conformation at high force to a different energy surface at lower force (Fig. 2 B). The protein monomer then diffuses along the new energy surface at low force until it eventually reaches its collapse length (Fig. 4). This experimental approach allows us to dissect and individually characterize the different stages encompassing the refolding trajectory of an unfolded protein (24). The richness encountered in the multiple stages of the folding reaction is hidden in the close-to-equilibrium trajectories obtained under constant-velocity trajectories, where both length and force are dynamically changing over time. Indeed, the study presented here using the out-of-equilibrium force-quench approach allows us to selectively study the collapse dynamics of a mechanically unfolded protein from a highly extended conformation

down to its collapse length. The final folding transition occurs at a much later time, when the ensemble of collapsed states formed after enthalpic collapse matures into the native state through a barrier-limited transition (37).

The theory and simulations demonstrated here now fully explain, in detail, the collapse trajectories observed during force-quench experiments on single proteins (15,16), validating force-clamp spectroscopy as a powerful tool for probing the free-energy landscape of a protein. Our analysis shows that from a small ensemble of force-quench trajectories, it is possible to measure the height and force dependence of the energy barrier between the entropic and enthalpic minima, the curvature of the free-energy minima, and the depth of the enthalpic minimum, and to determine the location of the transition states along the end-to-end coordinate. We are optimistic that faster force-clamp instrumentation coupled with novel force-pulse protocols will yield a complete reconstruction of the free energy of a folding protein. Once the full details of the free energy of a protein are known, solutions of the Langevin equation provide accurate representations of protein dynamics for an unlimited range of perturbations. This will prove useful in understanding the dynamics of elastic proteins like the giant muscle protein titin, exposed to fast and complex mechanical perturbations during the flapping of wings, jumps, and other types of animal behavior.

APPENDIX

Analytical derivation of the energy barrier governing protein collapse

One of the main findings reported in our work is the analytical derivation of the expression corresponding to the force-dependent energy barrier to collapse, ΔE , which results from the superposition of the entropic elasticity of the molecule combined with shorter-range enthalpic interactions. Both contributions have been identified as the principal contributors to the free energy of proteins collapsing under force. Such a derivation is described by Eq. 6, reported in the main text. To derive this equation, we approximated a potential profile in the vicinity of the transition area by a cubic function, as suggested in previous works (26,27,30). In such a way, the equation includes both the barrier and the entropic minimum. The original potential, U , given by Eqs. 1–4 in the main text, is approximated by

$$U(x) = U(x_0) + U'(x_0)(x - x_0) + \frac{U''(x_0)}{6}(x - x_0)^3, \quad (\text{A1})$$

where x_0 is a length at which $U'(x_0) = U''(x_0) = 0$. An equation for x_0 reads

$$\begin{aligned} & \left[\frac{k_B T}{8U} \right] \left[\frac{R_C^2}{b^2 P L_C} \right] \left[\frac{1}{2} (1 - y_0)^{-3} + 1 \right] \\ & = e^{-2 \frac{b}{R_C} R_C (y_0 \frac{L_C}{R_C} - 1)} - 2 e^{-4 \frac{b}{R_C} R_C (y_0 \frac{L_C}{R_C} - 1)}, \end{aligned} \quad (\text{A2})$$

where $y_0 = x_0/L_C$. Introducing the dimensionless parameters

$$\beta = \frac{L_C}{R_C} \text{ and } \alpha = \frac{k_B T}{8U} \frac{R_C^2}{b^2 P L_C}, \quad (\text{A3})$$

we can rewrite Eq. A2 as

$$\frac{\alpha}{2}(1 - y_0)^{-3} + \alpha = e^{-2b(\beta y_0 - 1)} - 2e^{-4b(\beta y_0 - 1)}. \quad (\text{A4})$$

It should be noted that under realistic conditions (such as those taken in the simulations), $\alpha \sim 3.2 \times 10^{-5}$ and $\beta \sim 10$. Under these conditions, Eq. A4 can be simplified and rewritten as

$$\alpha \sim e^{-2b(\beta y_0 - 1)}. \quad (\text{A5})$$

That gives

$$x_0 \sim \frac{L_C}{2b\beta}[2b - \ln(\alpha)] \text{ and } y_0 \sim \frac{2b - \ln(\alpha)}{2b\beta}. \quad (\text{A6})$$

Introducing the notations

$$\gamma = b\beta = b\frac{L_C}{R_C} \text{ and } \phi = 2b - \ln(\alpha), \quad (\text{A7})$$

we can rewrite x_0 as

$$x_0 \sim \frac{L_C}{2\gamma}\phi. \quad (\text{A8})$$

For the values of the parameters used in this article, Eq. A8 gives $x_0 = 10.7$ nm. Numerical calculations support the above approximation, giving $x_0^N = 10.0$ nm.

Using Eq. A1, we can find the height of the potential barrier:

$$\Delta E(F) = U(x_{\max}) - U(x_{\min}), \quad (\text{A9})$$

where x_{\min} and x_{\max} are the positions of the entropic minima and the maximum of the barrier, which can be calculated as:

$$x_{\min/\max} = x_0 \pm \sqrt{\frac{2U'(x_0)}{U'''(x_0)}} \quad (\text{A10})$$

Finally, we arrive at the equation for the force-dependent barrier height:

$$\Delta E = \varepsilon(F - F_C)^{3/2}, \quad (\text{A11})$$

where

$$\varepsilon = \left[\frac{3k_B T}{4PL_C^2} \left(\frac{2bL_C}{R_C} \right)^4 + \frac{k_B T b}{PR_C L_C} \right]^{-1/2}$$

$$\left(\frac{2bL_C}{R_C} - 2b + \ln \left(\frac{k_B T}{8U} \frac{R_C^2}{b^2 PL_C} \right) \right)$$

and

$$F_C = \frac{k_B T}{4P} \left[\left(\frac{2bL_C}{R_C} \right)^2 - 1 + \frac{4R_C}{L_C} \right. \\ \left. - \ln \left(\frac{k_B T}{8U} \frac{R_C^2}{b^2 PL_C} \right) \right] + \frac{k_B T}{2} \frac{R_C}{PbL_C}.$$

The force-dependent height of the barrier determines the distribution of collapse times and the mean collapse time measured in our experiments. The distribution is described by the equation

$$P(t) = ke^{-kt}, \quad (\text{A12})$$

where k is the transition rate,

$$k = k_0 e^{-\frac{\Delta E}{k_B T}}, \quad (\text{A13})$$

and k_0 is a prefactor. The mean time to collapse reads

$$\langle t \rangle = \frac{1}{k_0} e^{\frac{\Delta E(F)}{k_B T}}. \quad (\text{A14})$$

Another characteristic measured experimentally is the probability of leaving the entropic minimum and fully collapsing within the time frame of the experiment, Δt . It can be written as

$$P_{col}(F) = 1 - S, \quad (\text{A15})$$

where S is the survival probability of staying in the entropic well, which is a solution of the kinetic equation

$$\frac{dS}{dt} = -kS. \quad (\text{A16})$$

Then, for P_{col} , we have

$$P_{col} = 1 - e^{-\left(k_0 e^{-\frac{\Delta E(F)}{k_B T}}\right) \Delta t}. \quad (\text{A17})$$

This work was supported by the European Science Foundation EURO-CORES Program FANAS (collaborative research projects ACOF and AQUALUBE), International Science Foundation grant 1109/09 (to M.U. and J.K.), and National Institutes of Health grants HL66030 and HL61228 (to J.M.F.). S.G.-M. thanks the Fundación Caja Madrid for financial support.

REFERENCES

1. Mayor, U., N. R. Guydosh, ..., A. R. Fersht. 2003. The complete folding pathway of a protein from nanoseconds to microseconds. *Nature*. 421:863–867.
2. Sali, A., E. Shakhnovich, and M. Karplus. 1994. How does a protein fold? *Nature*. 369:248–251.
3. Onuchic, J. N., and P. G. Wolynes. 2004. Theory of protein folding. *Curr. Opin. Struct. Biol.* 14:70–75.
4. Dill, K. A., and H. S. Chan. 1997. From Levinthal to pathways to funnels. *Nat. Struct. Biol.* 4:10–19.
5. Schuler, B., E. A. Lipman, and W. A. Eaton. 2002. Probing the free-energy surface for protein folding with single-molecule fluorescence spectroscopy. *Nature*. 419:743–747.
6. Rhoades, E., E. Gussakovsky, and G. Haran. 2003. Watching proteins fold one molecule at a time. *Proc. Natl. Acad. Sci. USA*. 100:3197–3202.
7. Hoffmann, A., A. Kane, ..., B. Schuler. 2007. Mapping protein collapse with single-molecule fluorescence and kinetic synchrotron radiation circular dichroism spectroscopy. *Proc. Natl. Acad. Sci. USA*. 104:105–110.
8. Rief, M., M. Gautel, ..., H. E. Gaub. 1997. Reversible unfolding of individual titin immunoglobulin domains by AFM. *Science*. 276:1109–1112.
9. Carrion-Vazquez, M., A. F. Oberhauser, ..., J. M. Fernandez. 1999. Mechanical and chemical unfolding of a single protein: a comparison. *Proc. Natl. Acad. Sci. USA*. 96:3694–3699.
10. Schlierf, M., H. Li, and J. M. Fernandez. 2004. The unfolding kinetics of ubiquitin captured with single-molecule force-clamp techniques. *Proc. Natl. Acad. Sci. USA*. 101:7299–7304.

11. Jacob, J., B. Krantz, ..., T. R. Sosnick. 2004. Early collapse is not an obligate step in protein folding. *J. Mol. Biol.* 338:369–382.
12. Kohn, J. E., I. S. Millett, ..., K. W. Plaxco. 2004. Random-coil behavior and the dimensions of chemically unfolded proteins. *Proc. Natl. Acad. Sci. USA.* 101:12491–12496.
13. Walther, K. A., F. Gräter, ..., J. M. Fernandez. 2007. Signatures of hydrophobic collapse in extended proteins captured with force spectroscopy. *Proc. Natl. Acad. Sci. USA.* 104:7916–7921.
14. Brujic, J., R. I. Hermans, ..., J. M. Fernandez. 2006. Single-molecule force spectroscopy reveals signatures of glassy dynamics in the energy landscape of ubiquitin. *Nat. Phys.* 2:282–286.
15. Fernandez, J. M., and H. Li. 2004. Force-clamp spectroscopy monitors the folding trajectory of a single protein. *Science.* 303:1674–1678.
16. Garcia-Manyes, S., J. Brujic, ..., J. M. Fernández. 2007. Force-clamp spectroscopy of single-protein monomers reveals the individual unfolding and folding pathways of I27 and ubiquitin. *Biophys. J.* 93:2436–2446.
17. Brujic, J., and J. W. Fernandez. 2005. Response to comment on “Force-clamp spectroscopy monitors the folding trajectory of a single protein”. *Science.* 308:498c.
18. Thirumalai, D. 1995. From minimal models to real proteins: time scales for protein-folding kinetics. *J. Phys. I.* 5:1457–1467.
19. Best, R. B., and G. Hummer. 2005. Comment on “Force-clamp spectroscopy monitors the folding trajectory of a single protein”. *Science.* 308:498b.
20. Sosnick, T. R. 2004. Comment on “Force-clamp spectroscopy monitors the folding trajectory of a single protein”. *Science.* 306: 411, author reply 411.
21. Wright, C. F., S. A. Teichmann, ..., C. M. Dobson. 2005. The importance of sequence diversity in the aggregation and evolution of proteins. *Nature.* 438:878–881.
22. Borgia, A., P. M. Williams, and J. Clarke. 2008. Single-molecule studies of protein folding. *Annu. Rev. Biochem.* 77:101–125.
23. Li, P. T., D. Collin, ..., I. Tinoco, Jr. 2006. Probing the mechanical folding kinetics of TAR RNA by hopping, force-jump, and force-ramp methods. *Biophys. J.* 90:250–260.
24. Hyeon, C., G. Morrison, ..., D. Thirumalai. 2009. Refolding dynamics of stretched biopolymers upon force quench. *Proc. Natl. Acad. Sci. USA.* 106:20288–20293.
25. Gräter, F., P. Heider, ..., B. J. Berne. 2008. Dissecting entropic coiling and poor solvent effects in protein collapse. *J. Am. Chem. Soc.* 130: 11578–11579.
26. Tshiprut, Z., and M. Urbakh. 2009. Exploring hysteresis and energy dissipation in single-molecule force spectroscopy. *J. Chem. Phys.* 130:084703.
27. Tshiprut, Z., J. Klafter, and M. Urbakh. 2008. Single-molecule pulling experiments: when the stiffness of the pulling device matters. *Biophys. J.* 95:L42–L44.
28. Li, M. S., C. K. Hu, ..., D. Thirumalai. 2006. Multiple stepwise refolding of immunoglobulin domain I27 upon force quench depends on initial conditions. *Proc. Natl. Acad. Sci. USA.* 103:93–98.
29. Bustamante, C., J. F. Marko, ..., S. Smith. 1994. Entropic elasticity of lambda-phage DNA. *Science.* 265:1599–1600.
30. Dudko, O. K., A. E. Filippov, ..., M. Urbakh. 2003. Beyond the conventional description of dynamic force spectroscopy of adhesion bonds. *Proc. Natl. Acad. Sci. USA.* 100:11378–11381.
31. Risken, H. 1989. *The Fokker-Planck Equation, Methods of Solution and Applications.* Springer-Verlag, Berlin.
32. Li, H., A. F. Oberhauser, ..., J. M. Fernandez. 2001. Multiple conformations of PEVK proteins detected by single-molecule techniques. *Proc. Natl. Acad. Sci. USA.* 98:10682–10686.
33. Liu, R., S. Garcia-Manyes, ..., J. M. Fernández. 2009. Mechanical characterization of protein L in the low-force regime by electromagnetic tweezers/evanescent nanometry. *Biophys. J.* 96:3810–3821.
34. Cecconi, C., E. A. Shank, ..., S. Marqusee. 2005. Direct observation of the three-state folding of a single protein molecule. *Science.* 309: 2057–2060.
35. Schlierf, M., and M. Rief. 2009. Surprising simplicity in the single-molecule folding mechanics of proteins. *Angew. Chem. Int. Ed. Engl.* 48:820–822.
36. Best, R. B., and G. Hummer. 2008. Protein folding kinetics under force from molecular simulation. *J. Am. Chem. Soc.* 130:3706–3707.
37. Garcia-Manyes, S., L. Dougan, ..., J. M. Fernández. 2009. Direct observation of an ensemble of stable collapsed states in the mechanical folding of ubiquitin. *Proc. Natl. Acad. Sci. USA.* 106:10534–10539.